

Trifluoperazine prevents FOXO1 nuclear excretion and reverses doxorubicin-resistance in the SHG44/DOX drug-resistant glioma cell line

XIAOZHONG CHEN¹, XIAOQUAN LUO² and YUAN CHENG¹

¹Department of Neurosurgery, The Second Affiliated Hospital of Chongqing Medical University, Chongqing 400010; ²Department of Neurosurgery, Nanchong Central Hospital, Second Affiliated Hospital of North Sichuan Medical College, Nanchong, Sichuan 637000, P.R. China

Received January 6, 2018; Accepted September 4, 2018

DOI: 10.3892/ijmm.2018.3885

Abstract. As a tumor suppressor, Forkhead box O1 (FOXO1) is located in the nucleus where it regulates gene expression and inhibits tumor progression. However, the antitumor effects of FOXO1 are attenuated in several tumors due to its translocation from the nucleus to the cytoplasm. Trifluoperazine (TFP) is able to reverse tumor drug resistance by inhibiting multidrug resistance (MDR), however, the detailed molecular mechanisms by which this occurs remain to be fully elucidated. In the present study, the doxorubicin (DOX)-resistant SHG44/DOX glioma cell line was established. The results showed that TFP promoted DOX-induced cytotoxicity, cell cycle arrest and early apoptosis using a Cell Counting Kit-8 and flow cytometry. *In vivo* experiments also demonstrated that DOX combined with TFP reduced tumor volumes and proliferation indices, and led to higher protein levels of FOXO1. In addition, TFP inhibited the nuclear exclusion of FOXO1, contributing toward the downregulation of MDR genes and an increase in intracellular DOX concentrations by reverse transcription-quantitative polymerase chain reaction, western blot analysis, immunofluorescence and spectrophotometer analysis. Therefore, TFP may inhibit DOX resistance by stimulating FOXO1 nuclear translocation and suppressing MDR genes in SHG44/DOX cells, contributing to promising clinical prospects for tumor chemotherapy.

Introduction

Malignant gliomas are a life-threatening form of primary brain cancer characterized by uncontrollable and infiltrative growth that destroys surrounding normal brain tissues and causes neurological deficits (1). Following maximal surgical tumor excision, the standard treatment is chemo-radiotherapy. Despite multidisciplinary treatment approaches, gliomas have a high rate of recurrence, with few patients surviving >1 year (2). The failure of current therapeutics is partly attributed to drug resistance. Therefore, it is critical to focus on identifying novel target genes and the molecular mechanisms involved in the restoration of drug sensitivity (3).

Forkhead box O1 (FOXO1) belongs to the FOXO family of transcription factors, which are characterized by a conserved winged-helix DNA binding domain (4). The gene encoding FOXO1 is located at chromosome 13q14, where methylation, mutation and allelic losses are common occurrences in the presence of cancer. These characteristics suggest that there are potential tumor-associated genes involved in the origination and progression of human malignancies harbored in this region (5,6). Increasing evidence has demonstrated that FOXO1 is downregulated in several types of cancer with adverse outcomes (7). In addition, FOXO1 proteins are usually accumulated in the nucleus and act as a transcriptional regulator in non-tumor tissues. Once FOXO1 is phosphorylated in tumors, its proteins can migrate to the cytoplasm and become inactive, eliminating the expression of certain anticancer genes and leading to tumorigenesis (8). FOXO1 is able to inhibit tumor growth and has been identified as a tumor suppressor gene (TSG). Previous studies have shown that FOXO1 inhibited proliferation, prevented invasion and induced apoptosis in gliomas (9). Other data have also provided evidence that FOXO1 reversed chemotherapy resistance in certain types of cancer (10), however, this function in glioma remains to be fully elucidated.

Multidrug resistance (MDR) is a major barrier to radiotherapy and chemotherapy in cancer cells. A variety of mechanisms induce MDR phenotypes, however, the upregulation of ATP-binding cassette transporters represents the most common factor involved in MDR development (11).

Correspondence to: Professor Yuan Cheng, Department of Neurosurgery, The Second Affiliated Hospital of Chongqing Medical University, 74 Linjiang Road, Yuzhong, Chongqing 400010, P.R. China
E-mail: chengyuan023@aliyun.com

Key words: glioma, trifluoperazine, doxorubicin, Forkhead box O1, multidrug resistance

Trifluoperazine (TFP) is a phenothiazine derivative and is widely used as an antipsychotic drug. TFP may be clinically potent as a calmodulin antagonist and an inhibitor of the dopamine receptor (12). It has been reported that TFP reverses drug resistance in tumors through the inhibition of MDR genes, including P-glycoprotein (P-gp) (13). Of note, the anticancer effects of doxorubicin (DOX), bleomycin and gefitinib were found to be reinforced when TFP was combined with them (13-15). This suggests that TFP may be a valuable tool in overcoming MDR in cancer.

In the present study, the effects of FOXO1 on MDR phenotypes in glioma cells were examined. The data indicated that FOXO1 is a TSG, and that the nuclear translocation of FOXO1 was conducive for exerting anticancer functions. It was also confirmed that TFP may overcome drug resistance by limiting the nuclear excretion of FOXO1 in gliomas. This identification may accelerate TFP as a molecular therapy for gliomas.

Materials and methods

Reagents. The glioma SHG44 cell line was from Shanghai Life Academy of Sciences Cell Library (Shanghai, China). RPMI-1640 medium and fetal bovine serum (FBS) were obtained from Gibco; Thermo Fisher Scientific, Inc. (Waltham, MA, USA). Penicillin and streptomycin were purchased from HyClone; GE Healthcare Life Sciences (Logan, UT, USA). Primary antibodies targeting P-glycoprotein (P-gp, cat. no. sc-13131), multidrug resistance-associated protein 1 (MRP1, cat. no. sc-18835), lung resistance protein (LRP, cat. no. sc-23916), Ki67 nuclear antigen (Ki67, cat. no. sc-15402), and proliferating cell nuclear antigen (PCNA, cat. no. sc-25280) were purchased from Santa Cruz Biotechnology, Inc. (San Francisco, CA, USA). Antibodies targeting FOXO1 (cat. no. ab52857), α -tubulin (cat. no. ab18251) and Lamin B1 (cat. no. ab133741) were purchased from Abcam (Cambridge, MA, USA). Horseradish peroxidase (cat. no. ZB2301) or TRITC-conjugated (cat. no. ZF0313) secondary antibodies were purchased from Zhongshan Golden Bridge Biotechnology (Beijing, China). Epidermal growth factor (EGF), DAPI, RNase, propidium iodide (PI), the Annexin V-PE/7-AAD apoptosis reagent kit and TFP were purchased from Sigma; EMD Millipore (Billerica, MA, USA). The caspase-3 activity assay kit (cat. no. 12012952001) was purchased from Roche Diagnostics GmbH (Mannheim, Germany). DOX (cat. no. D1515; Sigma-Aldrich; Merck KGaA, Darmstadt, Germany). The RNAiso Plus, primescript RT reagent kit and DNA polymerase were purchased from Takara Biotechnology Co., Ltd. (Dalian, China). Cell Counting Kit-8 (CCK8), BSA, bicinchoninic acid (BCA) kit and the protein extraction kits (total, nuclear and cytosolic) were purchased from Beyotime Institute of Biotechnology (Beijing, China).

Cell culture. The human glioma SHG44 cell line and the DOX-resistant SHG44 cell line (SHG44/DOX) have been described previously (16). In brief, the SHG44 cells were maintained in a 5% CO₂ atmosphere at 37°C in RPMI-1640 medium supplemented with 100 U/ml penicillin, 100 mg/ml streptomycin and 10% FBS. The concentrations of DOX were gradually increased between 0.01 and 1 μ g/ml, resulting in the SHG44/DOX cells being able to grow in 0.1 μ g/ml DOX.

Reverse transcription-quantitative polymerase chain reaction (RT-qPCR) analysis. Total RNA was extracted from the cells using RNAiso Plus. The RNA sample concentrations were measured using a spectrophotometer and then reverse transcribed into cDNA using a primescript RT reagent kit. The primer sequences were as follows: MDR1 forward, 5'-CCC ATCATTGCAATAGCAGG-3' and reverse, 5'-GTTCAAAC TCTCTGCTGCTCCTGA-3'; MRP1 forward, 5'-GGCATC TCAGCAACTCGTCTT-3' and reverse, 5'-ATTAGCTTC CACGTCTCCTCCTT-3'; LRP forward, 5'-ACAAC TACT GCGTGATTCTC-3' and reverse, 5'-CTAGCATGTAGGTGC TTCCA-3'; and GAPDH forward, 5'-CTTTGGTATCGTGGA AGGACTC-3' and reverse, 5'-GTAGAGGCAGGGATGATG TTCT-3'. The reaction systems were as follows: The DNA polymerase 10 μ l, forward primer sequences (10 μ M) 0.8 μ l, reverse primer sequences (10 μ M) 0.8 μ l, cDNA 2.0 μ l and DEPC 6.4 μ l. The amplification conditions were as follows: 95°C for 30 sec, followed by 40 cycles at 95°C for 15 sec, and 60°C for 45 sec. The relative fold-changes in mRNA levels were calculated with the 2^{- $\Delta\Delta C_q$} method (17).

Western blot analysis. The nuclear, cytoplasmic and total proteins were extracted using their respective extraction kits according to the manufacturer's protocols. The protein concentrations were detected using the BCA method. An equal quantity (35 μ g) of each sample was separated by 6-12% SDS-PAGE and transferred onto PVDF membranes. The membranes were blocked with 5% goat serum for 1 h at 4°C and incubated with FOXO1 (dilution 1:200), P-gp (dilution 1:300), MRP1 (dilution 1:300), LRP (dilution 1:300), GAPDH (dilution 1:1,000), α -tubulin (dilution 1:500) and Lamin B1 (dilution 1:500) primary antibodies overnight at 4°C, and then washed with 5% TBST for three times and incubated with secondary antibody (dilution 1:5,000) for 1 h at 37°C. The membranes were then washed three times, and the protein in each band was quantified using Quantity One 4.6 computer software (Bio-Rad Laboratories, Inc., Hercules, CA, USA).

Immunofluorescence. The SHG44 and SHG44/DOX cells were collected to mount on the coverslip and fixed in 4% paraformaldehyde for 20 min. The cells were blocked with 5% BSA for 45 min then incubated with FOXO1 primary antibody (dilution 1:100) overnight at 4°C. The cells were then stained with a TRITC-labeled secondary antibody (1 h, dilution 1:500) and DAPI (4 min). The sections were coverslipped with 50% glycerol, and the location of the FOXO1 proteins was detected using a laser scanning confocal microscope (TCS SP2, Leica Microsystems GmbH, Wetzlar, Germany). For the negative control, 5% BSA was used in place of the primary antibodies.

Cell viability. The SHG44/DOX cells were divided into a blank group, a DOX group and a DOX + TFP group. The cells were grown in 96-well plates at a density of 2,000 cells/well. The cells were washed with PBS following various treatments (complete medium for blank group, 0.1 μ g/ml DOX for DOX group, 10 μ M TFP + 0.1 μ g/ml DOX for DOX + TFP group) for 24, 48 and 72 h. A total of 100 μ l medium and 10 μ l CCK-8 were added to each well for an additional 2 h. The absorbance values (OD values) were read at 450 nm using an enzyme-labeled instrument.

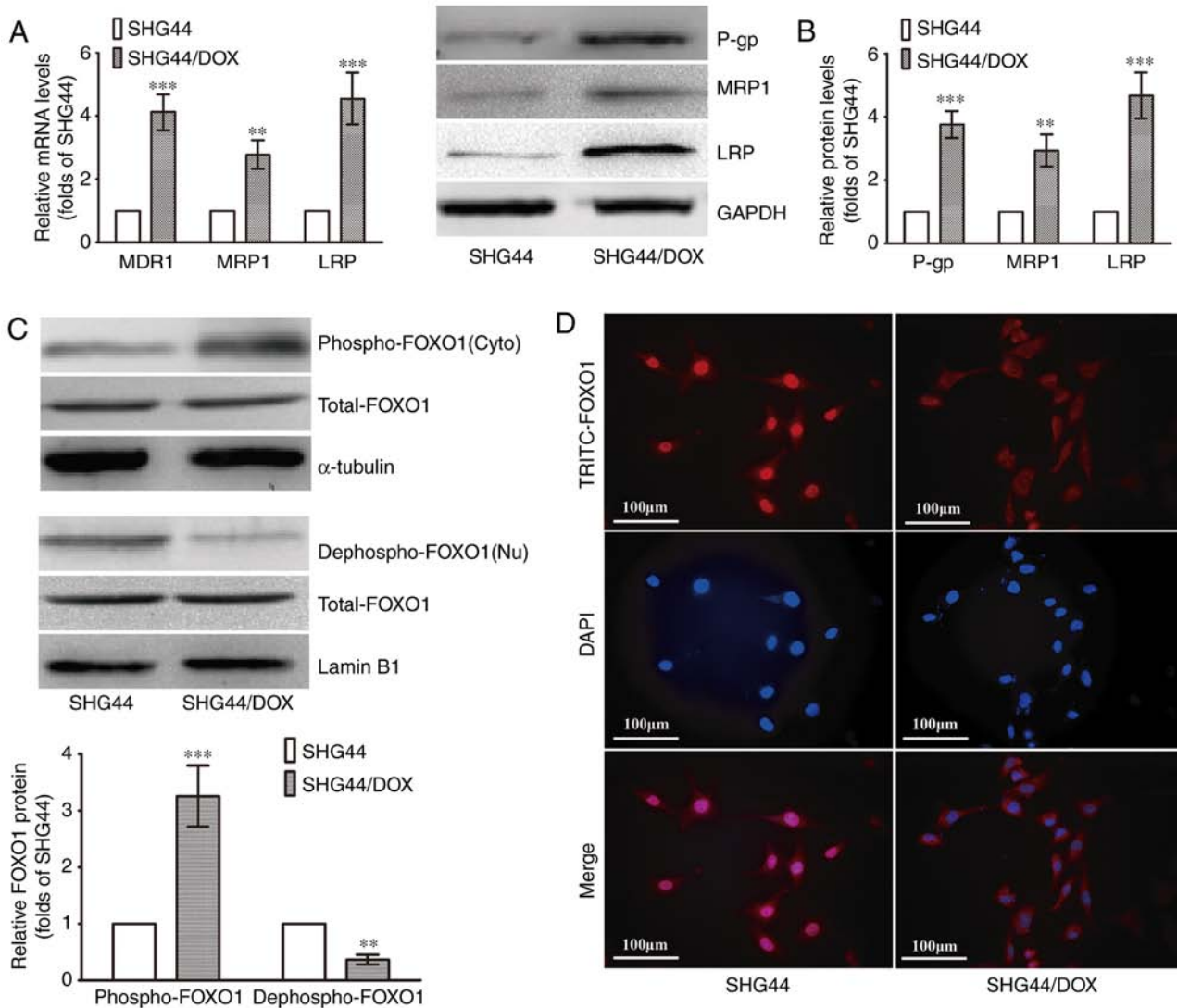


Figure 1. Expression of FOXO1 and MDR-associated molecules analyzed in SHG44 and SHG44/DOX glioma cells. (A) mRNA levels of MDR1, MRP1, LRP in SHG44 and SHG44/DOX cells. (B) Protein expression of P-gp, MRP1 and LRP in SHG44 and SHG44/DOX cells. (C) Western blot analysis was used to observe nuclear and cytoplasmic FOXO1 protein in the two cell lines. α -tubulin was the cytoplasmic protein loading control, and Lamin B1 was the nuclear protein loading control. (n=5, **P<0.01 and ***P<0.001, compared with SHG44). (D) Immunofluorescence for examining the location of FOXO1 proteins in the two cell lines. FOXO1, Forkhead box O1; DOX, doxorubicin; MDR, multidrug resistance; LRP, lung resistance protein; P-gp, P-glycoprotein; Nu, nuclear; Cyto, cytoplasmic.

Flow cytometry. For cell cycle distribution, 5×10^5 cells were harvested from each group and fixed in 70% ice-cold ethanol overnight. The cells were then treated with 10 mg/ml RNase and 50 mg/ml PI at 37°C for 30 min in the dark. The cell cycle distribution was analyzed by flow cytometry (BD Biosciences, Franklin Lakes, NJ, USA). Apoptosis was measured by flow cytometry using the Annexin V-PE/7-AAD apoptosis reagent kit according to the manufacturer's protocol. The SHG44/DOX cells from the blank group, the DOX group and the DOX + TFP group were harvested, re-suspended, and stained with phycoerythrin (PE)-labeled Annexin V and 7-aminoactinomycin D (7-AAD) for measuring early apoptosis.

Caspase-3 activity assay. To determine the intra-cellular caspase-3 activity in the SHG44/DOX control group, the DOX group and the DOX + TFP group, a commercial caspase-3 activity assay kit was utilized according to the manufacturer's protocol. The caspase-3 activities in implanted tumors were

also analyzed following injection with DOX or DOX + TFP. The values are presented as the percentage of the blank control.

DOX uptake. The SHG44/DOX cells were exposed to 0.1 µg/ml DOX, 0.1 µg/ml DOX + 10 µM TFP or 0.1 µg/ml DOX + 10 µM TFP + EGF for 2 h. Following cell lysis and supernatant collection, the intracellular concentrations of DOX were measured using a spectrophotometer (absorbance: 490 nm), and the protein concentrations were measured for standardizing the uptake of DOX.

Xenograft tumor model. All animal experiments were approved by the Ethics Committee of Chongqing Medical University (Chongqing, China). A total of 24 Male nude mice (4 weeks old, 14.4 ± 3.1 g) were provided by the Experimental Animal Center of Chongqing Medical University. The nude mice were housed in light for 10 h/day at 26°C. Food and

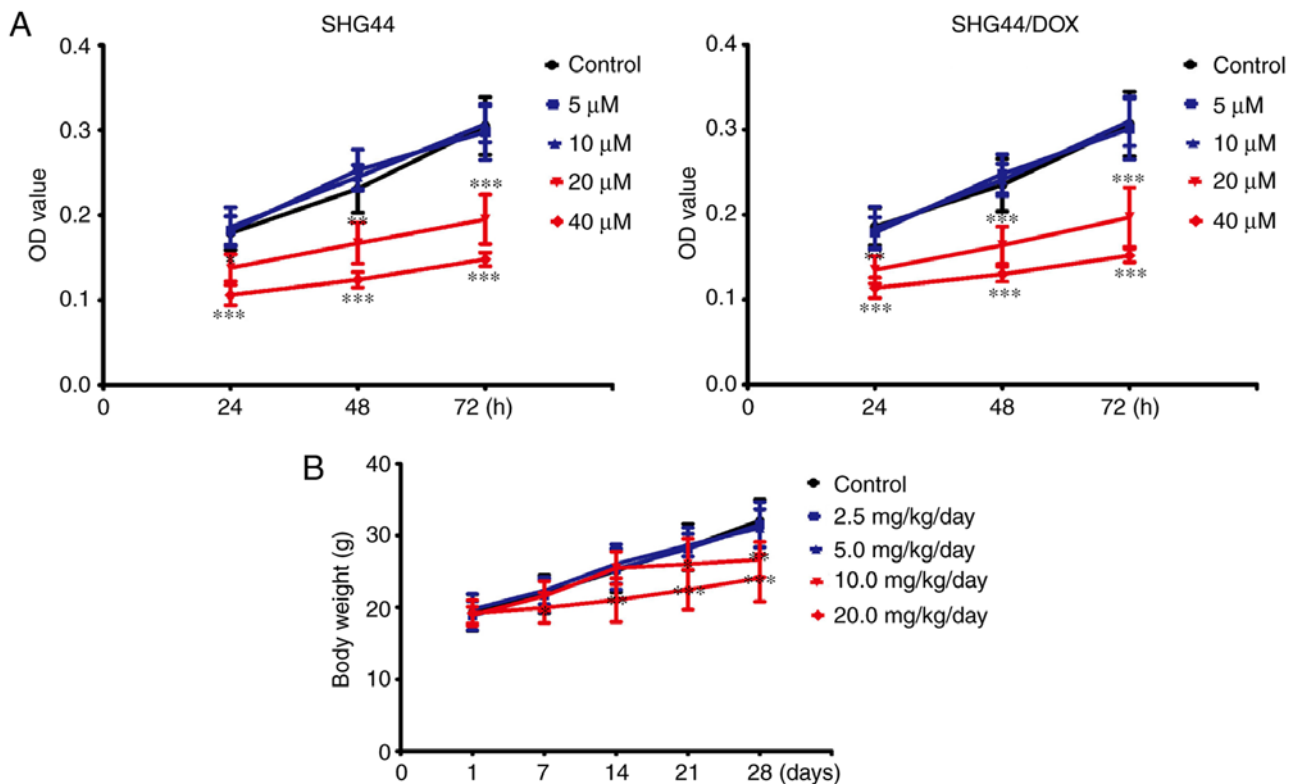


Figure 2. Assessment of TFP toxicity *in vitro* and *in vivo*. (A) CCK-8 for determining the cytotoxicity of TFP in SHG44 and SHG44/DOX cells (n=9). (B) Animal body weights of 4-week-old nude mice were measured following injection with various doses of TFP for 7, 14, 21, and 28 days (n=15 mice, n=3 experiments). *P<0.05, **P<0.01 and ***P<0.001, compared with the control group at the same time point. DOX, doxorubicin; TFP, trifluoperazine.

water were sterilized by high pressure steam and multivitamins were added into distilled water. The subcutaneous tumor model was produced as previously described (18). For treatment, 5 mg/kg DOX alone or 5 mg/kg DOX + 5 mg/kg/day TFP was injected the tail vein (DOX every 7 days and TFP every day). Tumor volumes were recorded at 7, 14, 21 and 28 days post-implantation in accordance with the previously described formula (18).

Immunohistochemistry (IHC). The mice were injected with 10% chloral hydrate (300 mg/kg) for anesthesia and sacrificed depending on cervical vertebra dislocation at 28 days. No mice exhibited signs of peritonitis. The tumor samples were dissected and embedded in paraffin. Paraffin-embedded sections (4 mm) were prepared and IHC procedures were performed based on prior methods (19). The proliferation indices of Ki-67 (dilution 1:100) and PCNA (dilution 1:100) were defined as the percentage of positive cells from five randomly selected fields at x400 magnification using a laser scanning confocal microscope (TCS SP2; Leica Microsystems GmbH, Wetzlar, Germany).

Statistical analysis. Statistical analyses were performed using SPSS 20.0 software (IBM SPSS, Armonk, NY, USA). Statistical differences among groups were analyzed by one-way analysis of variance and the Student-Neuman-Keuls post hoc test, two-sample t-test or χ^2 test. P<0.05 was considered to indicate a statistically significant difference. All data are presented as the mean \pm standard deviation.

Results

Downregulation of nuclear FOXO1 in SHG44/DOX cells. The SHG44/DOX cells were established according to previous methods. The RT-qPCR analysis showed that three MDR genes (MDR1, MRP1 and LRP) were upregulated in the SHG44/DOX cells compared with the SHG44 cells (Fig. 1A). The protein levels of P-gp, MRP1 and LRP were also increased in the SHG44/DOX cells, as determined by western blot analysis (Fig. 1B). The levels of nuclear FOXO1 (dephospho-FOXO1) were lower in the SHG44/DOX cells than in the SHG44 cells, whereas a higher expression of cytoplasmic FOXO1 (p-FOXO1) was detected in the SHG44/DOX cells (Fig. 1C). The immunofluorescence also verified that the FOXO1 proteins were excreted into the cytoplasm in SHG44/DOX cells (Fig. 1D). These data suggested that FOXO1 proteins were expressed in the cytoplasm, resulting in a loss of transcriptional activity and tumor inhibitory effects in the SHG44/DOX drug-resistant glioma cells.

Non-toxic concentrations of TFP *in vitro* and *in vivo*. To avoid toxicity from TFP in the SHG44 and SHG44/DOX cells, the appropriate dose of TFP was selected. Following treatment with concentrations of $\leq 10 \mu$ M for 24, 48, or 72 h, TFP did not inhibit growth of the two selected cell lines. However, TFP may reduce cell viability at a concentration of 20 μ M in SHG44 and SHG44/DOX cells (Fig. 2A). TFP toxicity surveys were performed *in vivo*. The mice were administered with 0, 2.5, 5, 10, or 20 mg/kg/day of TFP through tail vein injections. No changes in bodyweight were observed with administration

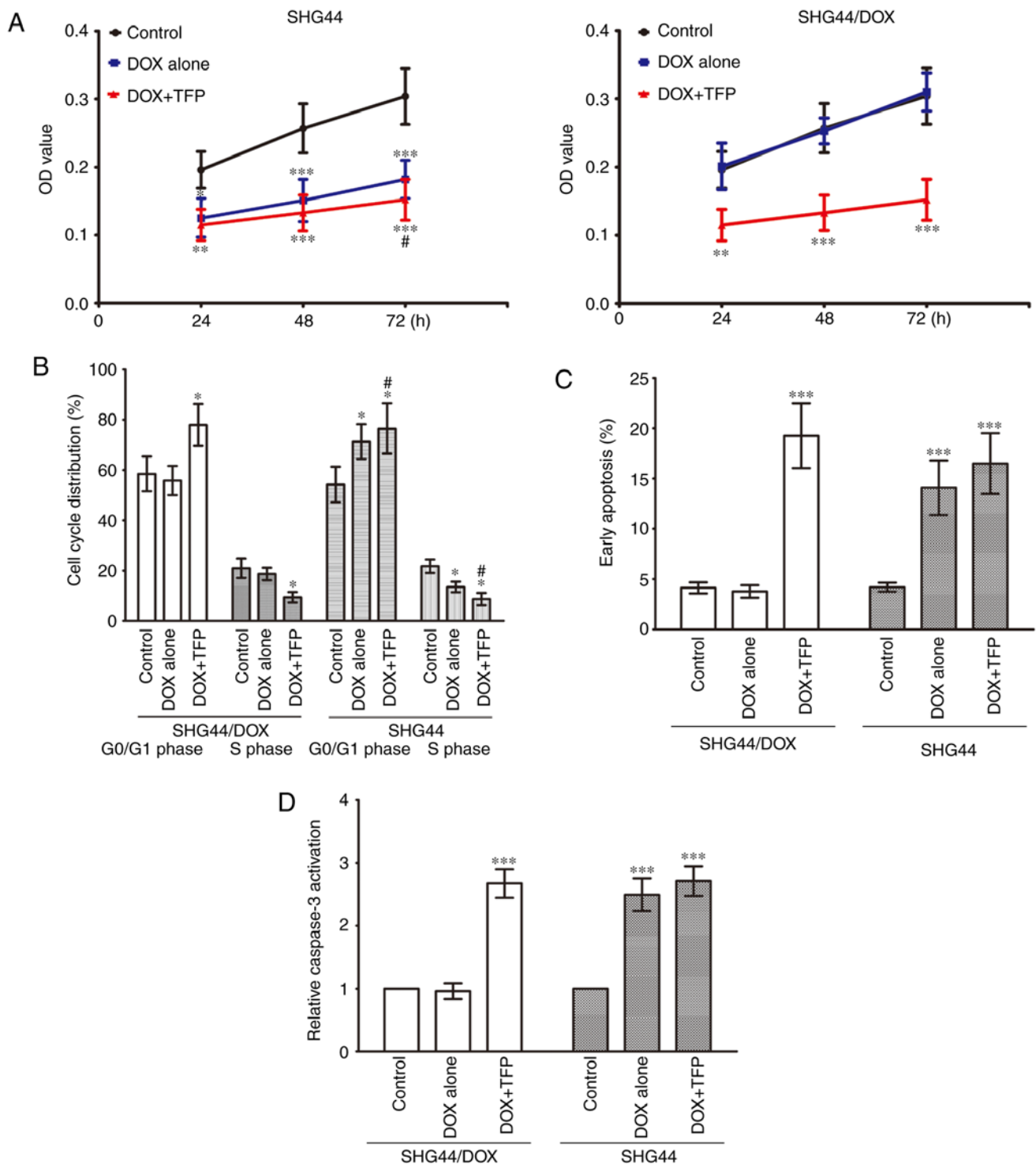


Figure 3. TFP restores the anticancer effects of DOX in SHG44/DOX cells *in vitro*. (A) CCK-8 was used to analyze SHG44 and SHG44/DOX cell growth following incubation with DOX or DOX + TFP for 24, 48, and 72 h (n=9). (B) Cell cycles were assessed and quantified in the blank control, DOX and DOX + TFP groups of SHG44 and SHG44/DOX cells by flow cytometry after 72 h (n=5). (C) Early apoptotic rates of SHG44 and SHG44/DOX cells were also detected in the three groups (n=5). (D) Caspase-3 activation was analyzed in the DOX + TFP groups and compared with the control group and DOX alone group (n=9). *P<0.05, **P<0.01 and ***P<0.001, vs. control group. #P<0.05, vs. DOX alone group. DOX, doxorubicin; TFP, trifluoperazine.

of 5 mg/kg/day within 4 weeks (Fig. 2B). Therefore, these non-toxic concentrations of TFP (10 μ M *in vitro* and 5 mg/kg/day *in vivo*) were used for the experiments.

TFP overcomes DOX-resistance in SHG44/DOX cells *in vitro*. The CCK-8 assay showed that the cell viability of the SHG44 cells was suppressed by 0.1 μ g/ml DOX, and

10 μ M TFP marginally promoted the growth inhibition effect of DOX at 72 h. The growth of SHG44/DOX cells was not inhibited by 0.1 μ g/ml DOX, however, 10 μ M TFP + 0.1 μ g/ml DOX prevented the growth of SHG44/DOX cells at 24, 48 and 72 h (Fig. 3A). Flow cytometry revealed that the percentage of G₀/G₁ phase cells was increased and the percentage of S phase cells was decreased in the SHG44 group following

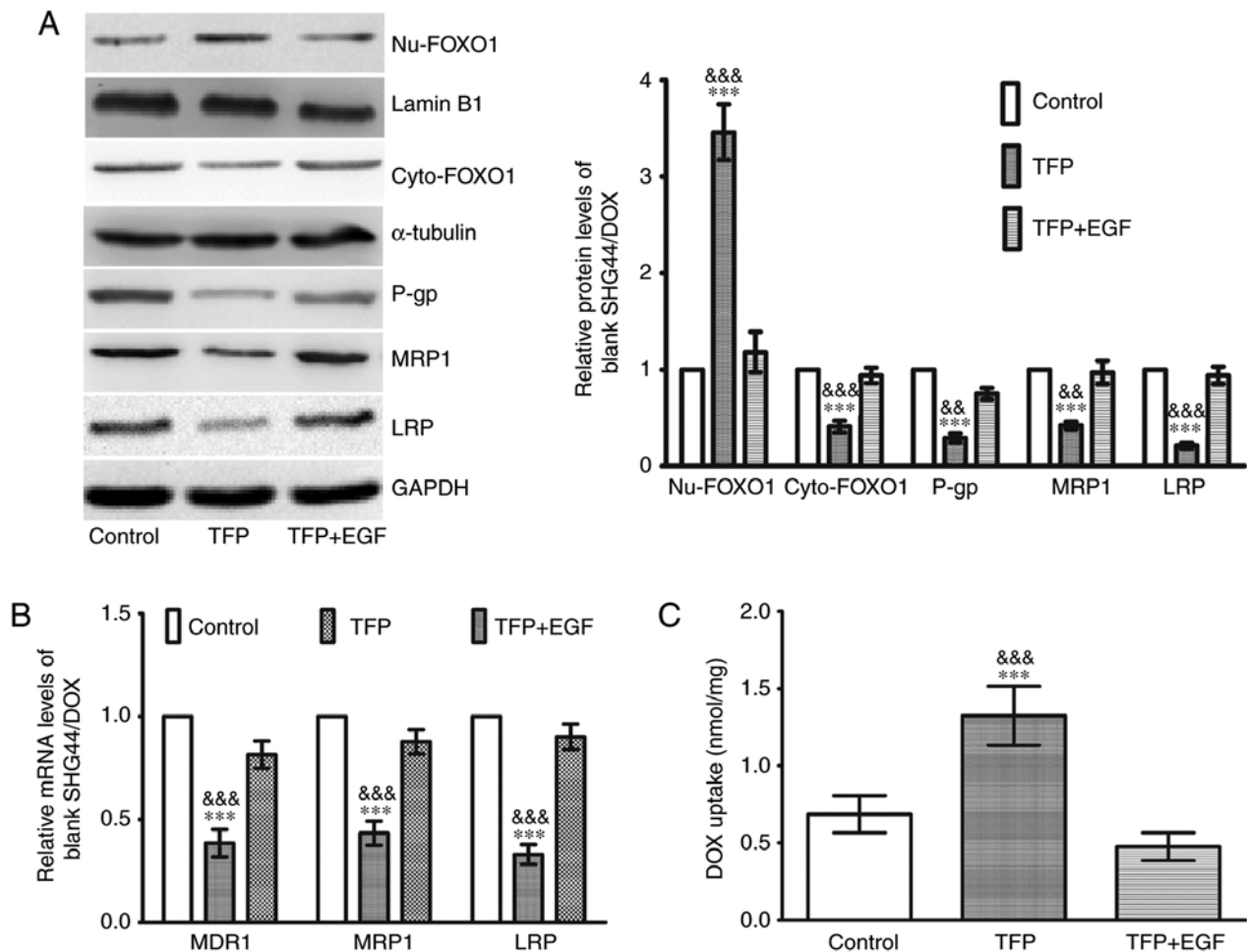


Figure 4. TFP induces DOX uptake in SHG44/DOX cells through the inhibition of FOXO1 nuclear exclusion and MDR genes. (A) Following treatment with TFP or TFP + EGF for 24 h, western blot analysis showed that TFP reduced the protein levels of P-gp, MRP1, and LRP by upregulating nuclear FOXO1 in SHG44/DOX cells (n=5). (B) Reverse transcription-quantitative polymerase chain reaction analysis was used to observe the effects of TFP on mRNA levels of MDR1, MRP1 and LRP in SHG44/DOX cells (n=5). (C) Following incubation with DOX (0.1 μ g/ml) for 2 h, spectrophotometry was used to measure intracellular concentrations of DOX in the control, TFP and TFP + EGF groups (n=5). ***P<0.001, vs. control; &&P<0.01 and &&&P<0.001, vs. TFP + EGF group). FOXO1, Forkhead box O1; MDR, multidrug resistance; DOX, doxorubicin; TFP, trifluoperazine; P-gp, P-glycoprotein; MRP1, multidrug resistance-associated protein 1; LRP, lung resistance protein; EGF, epidermal growth factor; Nu, nuclear; Cyto, cytoplasmic.

treatment with 0.1 μ g/ml DOX. However, these effects were more pronounced when 10 μ M TFP was added. Treatment with 0.1 μ g/ml DOX did not alter cell cycle distribution in SHG44/DOX cells; however, the percentage of G₀/G₁ phase cells was higher in the 10 μ M TFP + 0.1 μ g/ml DOX group than in the control group and the 0.1 μ g/ml DOX group, whereas the percentage of S phase cells was lower in the 10 μ M TFP + 0.1 μ g/ml DOX group than in the other two groups (Fig. 3B). Furthermore, 0.1 μ g/ml DOX induced early apoptosis in SHG44 cells, but this did not occur in the SHG44/DOX cells. DOX did accelerate early apoptosis and caspase-3 activities in SHG44/DOX cells at 72 h when it was combined with 10 μ M TFP (Fig. 3C and D).

TFP decreases MDR genes and facilitates DOX uptake through restoration of the nuclear localization of FOXO1 in SHG44/DOX cells. Western blot analysis was used to elucidate the molecular mechanisms involved in the effects of TFP inhibition of DOX drug-resistance. As shown in Fig. 4A, there was an increase in nuclear FOXO1 and a decrease in cytoplasmic FOXO1 in the 10 μ M TFP group, coupled with

a downregulation of P-gp, MRP1 and LRP. EGF stimulates FOXO1 nuclear exclusion (20). When EGF was added to the TFP group, the TFP-induced FOXO1 nuclear accumulation was counteracted, and the levels of the three MDR proteins were increased (Fig. 4A). The changes in the mRNA expression of MDR1, MRP1 and LRP were consistent with their protein expression (Fig. 4B). Following treatment with 0.1 μ g/ml DOX, 0.1 μ g/ml DOX + 10 μ M TFP, or 0.1 μ g/ml DOX + 10 μ M TFP + EGF for 2 h, the intracellular concentrations of DOX were assessed. Spectrophotometer analysis revealed that 10 μ M TFP was able to enhance the intracellular concentrations of DOX in SHG44/DOX cells. However, EGF restored the expression of MDR proteins and contributed to DOX excretion from the glioma cells (Fig. 4C).

DOX-resistance of SHG44/DOX cells is attenuated by TFP *in vivo*. The efficacy of TFP on the enhanced cell toxicity of DOX was examined in subcutaneous xenotransplanted tumors. Although 5 mg/kg DOX did not suppress the xenograft tumors, 5 mg/kg DOX + 5 mg/kg/day TFP reduced SHG44/DOX growth *in vivo* compared with that in the control group and

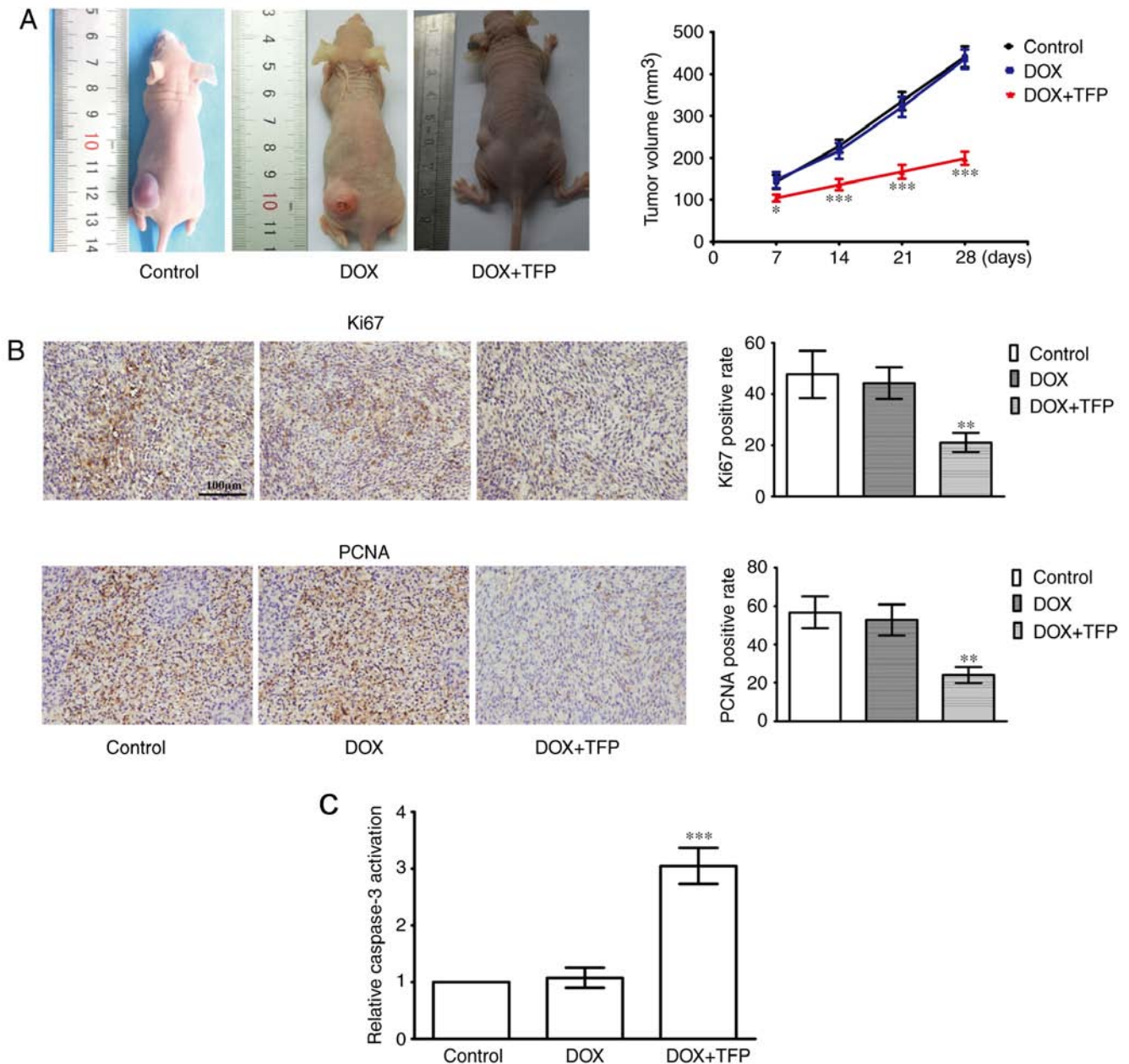


Figure 5. TFP inhibits DOX-resistance of SHG44/DOX *in vivo*. (A) Xenografted tumors were divided into a control group, DOX alone group and DOX + TFP group. The tumor volumes were calculated at 7, 14, 21 and 28 days (n=9 mice; n=3 experiments). (B) After 28 days, immunohistochemistry was used to observe the percent positive for PCNA and Ki67 in the tumor samples (magnification, x400). (C) Xenografted tumors derived from SHG44/DOX cells were collected to detect apoptosis using a caspase-3 activity assay. *P<0.05, **P<0.01 and ***P<0.001, compared with the control and DOX alone group. DOX, doxorubicin; TFP, trifluoperazine.

DOX alone group (Fig. 5A). IHC showed that the Ki-67 and PCNA proliferation indices were lower in the 5 mg/kg DOX + 5 mg/kg/day TFP group than that in the control group and the 5 mg/kg DOX alone group (Fig. 5B). In addition, the effect of DOX-induced apoptosis was also restored when TFP (5 mg/kg/day) was added (Fig. 5C).

Discussion

Numerous studies have reported that FOXO1 functions as a tumor suppressor and inhibits the development of different types of cancer, with FOXO1 inactivation being accompanied with a poor prognosis in patients (6,7). FOXO1 contains a

conserved DNA-binding domain and links to the consensus DNA-binding sequence (TTGTTTAC) of target genes (9). For example, FOXO1 makes contact with the p27 promoter, initiates transcription and suppresses cell cycle progression (21). FOXO1 also decreases tumor invasion by inhibiting matrix metalloproteinase (MMP)7, MMP9, vascular endothelial growth factor and hypoxia-inducible factor-1 α (22,23). However, the inactivation of FOXO1 has been noted to occur in several tumor types (24-26). FOXO1 has a direct effect in the Akt signaling pathway, which is active when malignancies are present. Akt phosphorylates FOXO1, resulting in nuclear exclusion and loss of binding to target regulatory elements (27,28). In the present study, it was demonstrated that

FOXO1 was conducive to enhancing chemotherapy sensitivity and indicated that it may be involved in glioma pathogenesis. It has been suggested that c-Jun N-terminal kinase is an upstream regulatory molecule of FOXO1 and may inhibit its activation, contributing to a tolerance for 5-fluorouracil and chemotherapy failure (29). Serum and glucocorticoid-regulated kinase isoform 1, extracellular signal-regulated kinase, inhibitor of nuclear factor- κ B kinase, and AMP-activated protein kinase have also been described as negative regulators of FOXO1 (30,31). Together, this suggests that FOXO1 is a convergence target for several signaling pathways and has an opposing role in tumorigenesis (32).

TFP is used as a neuroleptic for controlling psychotic disturbances, but it has also been reported to exert anticancer effects on several cancer cells. Studies have revealed that calmodulin antagonists can interfere with Ca^{2+} -calmodulin interactions, prevent Ca^{2+} -dependent cellular events and thereby limiting tumor growth (33). As a calmodulin antagonist, TFP also induces apoptosis and inhibits tumorigenesis, proliferation and metastasis in several tumor types (12,15). Furthermore, TFP is responsible for inactivating the dopamine receptor D2, and inhibiting angiogenesis and invasion (34). It has also been reported that TFP is able to prevent the phosphorylation and activation of Akt, which is an important molecular mechanism for oncotherapy. The inactive Akt enhances the nuclear translocation of FOXO1 and prevents tumor progression (34). Therefore, it was hypothesized that TFP is capable of inhibiting gliomas by modulating FOXO1. Data have suggested that TFP promotes the tumor inhibitory activity of FOXO1 (20). In the present study, it was also shown that TFP increased nuclear FOXO1 protein, decreased the levels of MDR genes, suppressed the efflux of DOX from glioma cells and restricted glioma growth. These results are consistent with those of other studies, which have confirmed that TFP may be useful as a chemotherapy adjuvant for gliomas and for reversing ATP binding cassette transporter-relevant MDR (13). The present study also found that the levels of breast cancer resistance protein (BCRP) in SHG44/DOX cells were not increased as much as the P-gp, MRP1 and LRP proteins (data not shown). The reason for this may involve the upregulation of P-gp in SHG44/DOX to result in the inhibition of BCRP. However, the levels of BCRP may have been increased when P-gp was inhibited. Therefore, it is important to emphasize that chemotherapy failure may occur if only P-gp levels are reduced, leading to BCRP being restored and becoming a candidate MDR mechanism.

In conclusion, FOXO1 appears to be a novel therapeutic target for MDR. TFP is conducive in regulating FOXO1 and downstream drug resistance genes, and restoring DOX-induced cytotoxicity. The present study provides the experimental basis for a clinical application of TFP to reverse glioma chemotherapy resistance and improve the efficacy of chemotherapeutic drugs for this disease. These results may assist in the development of a novel strategy for molecular cancer therapy for glioma.

Acknowledgements

Not applicable.

Funding

No funding was received.

Availability of data and materials

The datasets used and/or analyzed during the current study are available from the corresponding author on reasonable request.

Authors' contributions

YC designed the study. XL cultured the SHG44/DOX cell line and completed the xenograft tumor model. XC performed the *in vitro* and *in vivo* experiments. All authors read and approved the final manuscript.

Ethics approval and consent to participate

All animal experiments were approved by the Ethics Committee of Chongqing Medical University (Chongqing, China).

Patient consent for publication

Not applicable.

Competing interests

The authors declare that they have no competing interests.

References

1. Sontheimer H: Brain cancer: Tumour cells on neighbourhood watch. *Nature* 528: 49-50, 2015.
2. Geng F, Cheng X, Wu X, Yoo JY, Cheng C, Guo JY, Mo X, Ru P, Hurwitz B, Kim SH, *et al*: Inhibition of SOAT1 suppresses glioblastoma growth via blocking SREBP-1-mediated lipogenesis. *Clin Cancer Res* 22: 5337-5348, 2016.
3. Stupp R, Brada M, van den Bent MJ, Tonn JC, Pentheroudakis G, and ESMO Guidelines Working Group: High-grade glioma: ESMO clinical practice guidelines for diagnosis, treatment and follow-up. *Ann Oncol* 25: iii93-iii101, 2014.
4. Xu Y, Zhao S, Cui M and Wang Q: Down-regulation of microRNA-135b inhibited growth of cervical cancer cells by targeting FOXO1. *Int J Clin Exp Pathol* 8: 10294-10304, 2015.
5. Yamagata K, Daitoku H, Takahashi Y, Namiki K, Hisatake K, Kako K, Mukai H, Kasuya Y and Fukamizu A: Arginine methylation of FOXO transcription factors inhibits their phosphorylation by Akt. *Mol Cell* 32: 221-231, 2008.
6. Coomans de Brachène A and Demoulin JB: FOXO transcription factors in cancer development and therapy. *Cell Mol Life Sci* 73: 1159-1172, 2016.
7. Song HM, Song JL, Li DF, Hua KY, Zhao BK and Fang L: Inhibition of FOXO1 by small interfering RNA enhances proliferation and inhibits apoptosis of papillary thyroid carcinoma cells via Akt/FOXO1/Bim pathway. *Oncotargets Ther* 8: 3565-3573, 2015.
8. Li CF, Zhang WG, Liu M, Qiu LW, Chen XF, Ly L and Mei ZC: Aquaporin 9 inhibits hepatocellular carcinoma through up-regulating FOXO1 expression. *Oncotarget* 7: 44161-44170, 2016.
9. Cheng C, Jiao JT, Qian Y, Guo XY, Huang J, Dai MC, Zhang L, Ding XP, Zong D and Shao JF: Curcumin induces G2/M arrest and triggers apoptosis via FoxO1 signaling in U87 human glioma cells. *Mol Med Rep* 13: 3763-3770, 2016.
10. Shen H, Wang D, Li L, Yang S, Chen X, Zhou S, Zhong S, Zhao J and Tang J: MiR-222 promotes drug-resistance of breast cancer cells to adriamycin via modulation of PTEN/Akt/FOXO1 pathway. *Gene* 596: 110-118, 2017.
11. Arrighi E, Galimberti S, Pettrini M, Danesi R and Di Paolo A: ATP-binding cassette transmembrane transporters and their epigenetic control in cancer: An overview. *Expert Opin Drug Metab Toxicol* 12: 1419-1432, 2016.

12. Chen QY, Wu LJ, Wu YQ, Lu GH, Jiang ZY, Zhan JW, Jie Y and Zhou JY: Molecular mechanism of trifluoperazine induces apoptosis in human A549 lung adenocarcinoma cell lines. *Mol Med Rep* 2: 811-817, 2009.
13. Shin SY, Choi BH, Kim JR, Kim JH and Lee YH: Suppression of P-glycoprotein expression by antipsychotics trifluoperazine in adriamycin-resistant L1210 mouse leukemia cells. *Eur J Pharm Sci* 28: 300-306, 2006.
14. Polischouk AG, Holgersson A, Zong D, Stenerlöv B, Karlsson HL, Möller L, Viktorsson K and Lewensohn R: The antipsychotic drug trifluoperazine inhibits DNA repair and sensitizes non small cell lung carcinoma cells to DNA double-strand break induced cell death. *Mol Cancer Ther* 6: 2303-2309, 2007.
15. Yeh CT, Wu AT, Chang PM, Chen KY, Yang CN, Yang SC, Ho CC, Chen CC, Kuo YL, Lee PY, *et al*: Trifluoperazine, an antipsychotic agent, inhibits cancer stem cell growth and overcomes drug resistance of lung cancer. *Am J Respir Crit Care Med* 186: 1180-1188, 2012.
16. Chen J, Xu ZY and Wang F: Association between DNA methylation and multidrug resistance in human glioma SHG-44 cells. *Mol Med Rep* 11: 43-52, 2015.
17. Wen K, Fu Z, Wu X, Feng J, Chen W and Qian J: Oct-4 is required for an antiapoptotic behavior of chemoresistant colorectal cancer cells enriched for cancer stem cells: effects associated with STAT3/Survivin. *Cancer Lett* 333: 56-65, 2013.
18. Huang N, Cheng S, Mi X, Tian Q, Huang Q, Wang F, Xu Z, Xie Z, Chen J and Cheng Y: Downregulation of nitrogen permease regulator like-2 activates PDK1-AKT1 and contributes to the malignant growth of glioma cells. *Mol Carcinog* 55: 1613-1626, 2016.
19. Chen S, Zhao H, Deng J, Liao P, Xu Z and Cheng Y: Comparative proteomics of glioma stem cells and differentiated tumor cells identifies S100A9 as a potential therapeutic target. *J Cell Biochem* 114: 2795-2808, 2013.
20. Sangodkar J, Dhawan NS, Melville H, Singh VJ, Yuan E, Rana H, Izadmehr S, Farrington C, Mazhar S, Katz S, *et al*: Targeting the FOXO1/KLF6 axis regulates EGFR signaling and treatment response. *J Clin Invest* 122: 2637-2651, 2012.
21. Zhao Z, Qin L and Li S: miR-411 contributes the cell proliferation of lung cancer by targeting FOXO1. *Tumour Biol* 37: 5551-5560, 2016.
22. Ding H, Zhu Y, Chu T and Wang S: Epidermal growth factor induces FoxO1 nuclear exclusion to activate MMP7-mediated metastasis of larynx carcinoma. *Tumour Biol* 35: 9987-9992, 2014.
23. Pei J, Lou Y, Zhong R and Han B: MMP9 activation triggered by epidermal growth factor induced FoxO1 nuclear exclusion in non-small cell lung cancer. *Tumour Bio* 35: 6673-6678, 2014.
24. Myatt SS, Wang J, Monteiro LJ, Christian M, Ho KK, Fusi L, Dina RE, Brosens JJ, Ghaem-Maghamsi S and Lam EW: Definition of microRNAs that repress expression of the tumor suppressor gene FOXO1 in endometrial cancer. *Cancer Res* 70: 367-377, 2010.
25. Hou T, Ou J, Zhao X, Huang X, Huang Y and Zhang Y: MicroRNA-196a promotes cervical cancer proliferation through the regulation of FOXO1 and p27Kip1. *Br J Cancer* 110: 1260-1268, 2014.
26. Magro G, Righi A, Casorzo L, Antonietta T, Salvatorelli L, Kacerovská D, Kazakov D and Michal M: Mammary and vaginal myofibroblastomas are genetically related lesions: Fluorescence in situ hybridization analysis shows deletion of 13q14 region. *Hum Pathol* 43: 1187-1193, 2012.
27. Zhang X, Tang N, Hadden TJ and Rishi AK: Akt, FoxO and regulation of apoptosis. *Biochim Biophys Acta* 1813: 1978-1986, 2011.
28. Lian R, Lu B, Jiao L, Li S, Wang H, Miao W and Yu W: MiR-132 plays an oncogenic role in laryngeal squamous cell carcinoma by targeting FOXO1 and activating the PI3K/AKT pathway. *Eur J Pharmacol* 792: 1-6, 2016.
29. Altan B, Yokobori T, Ide M, Mochiki E, Toyomasu Y, Kogure N, Kimura A, Hara K, Bai T, Bao P, *et al*: Nuclear PRMT1 expression is associated with poor prognosis and chemosensitivity in gastric cancer patients. *Gastric Cancer* 19: 789-797, 2016.
30. Van Der Heide LP, Hoekman MF and Smidt MP: The ins and outs of FoxO shuttling: Mechanisms of FoxO translocation and transcriptional regulation. *Biochem J* 380: 297-309, 2004.
31. Zou J, Hong L, Luo C, Li Z, Zhu Y, Huang T, Zhang Y, Yuan H, Hu Y, Wen T, *et al*: Metformin inhibits estrogen-dependent endometrial cancer cell growth by activating the AMPK-FOXO1 signal pathway. *Cancer Sci* 107: 1806-1817, 2016.
32. Sun F, Han DF, Cao BQ, Wang B, Dong N and Jiang DH: Caffeine-induced nuclear translocation of FoxO1 triggers Bim-mediated apoptosis in human glioblastoma cells. *Tumour Biol* 37: 3417-3423, 2016.
33. Yuan K, Yong S, Xu F, Zhou T, McDonald JM and Chen Y: Calmodulin antagonists promote TRA-8 therapy of resistant pancreatic cancer. *Oncotarget* 6: 25308-25319, 2015.
34. Pulkoski-Gross A, Li J, Zheng C, Li Y, Ouyang N, Rigas B, Zucker S, Cao J: Repurposing the antipsychotic trifluoperazine as an antimetastasis agent. *Mol Pharmacol* 87: 501-512, 2015.



This work is licensed under a Creative Commons Attribution-NonCommercial-NoDerivatives 4.0 International (CC BY-NC-ND 4.0) License.